

Ion-etch produced damage on InAs(100) studied through collective-mode electronic Raman scattering

T. A. Tanzer and P. W. Bohn^{a)}

Department of Chemistry and Materials Research Laboratory, University of Illinois at Urbana-Champaign, 600 S. Mathews Avenue, Urbana, Illinois 61801

I. V. Roshchin and L. H. Green^{b)}

Department of Physics and Materials Research Laboratory, University of Illinois at Urbana-Champaign, 1110 W. Green Street, Urbana, Illinois 61801

(Received 8 July 1999; accepted 26 November 1999)

Raman scattering and x-ray photoelectron spectroscopy are used to study the damage induced by low energy Ar⁺ milling on InAs(100) surfaces. Evidence for etch-induced lattice damage is obtained even under the mildest conditions employed. Etching at 75 V creates an In-rich surface and reduces the intensity of scattering from the unscreened longitudinal optic (LO) phonon in the near-surface region. Etching at higher voltages creates damage states that increase the carrier concentration at depths at least as large as the Raman probe depth (~ 100 Å). Postetch annealing at 500 °C in ultrahigh vacuum restores the LO phonon mode to its original intensity, the carrier concentration to original levels, and a stoichiometric (In:As=1:1) surface composition. Etch-induced lattice damage in the near-surface region, which is subsequently removed by annealing at optimal temperatures, is the only mechanism consistent with all the inelastic light scattering and composition results. © 2000 American Vacuum Society. [S0734-211X(00)10201-X]

I. INTRODUCTION

InAs presents novel opportunities and challenges for device fabrication due to the narrow energy gap and unusual band bending at the surface.¹⁻⁸ In most III-V semiconductors, surface-induced band bending creates a surface depletion layer, which acts as a barrier to electron transport. In contrast, the band bending at InAs (100) and (110) surfaces leads to a charge accumulation region (CAR) in which the electron concentration is higher than in the bulk. Furthermore, at doping concentrations greater than $\sim 10^{17}$ cm⁻³, the Fermi level is above the conduction band minimum, causing degeneracy. This situation leads to ohmic contact formation and high transmittance metal-semiconductor interfaces.² These same properties make InAs an attractive material for the study of interfacial charge transport. Of particular interest in our laboratories is the study of charge transport in superconductor-semiconductor (S:Sm) interfaces near the superconducting critical temperature.⁹⁻¹¹ The first observation of an optical signature of the superconducting proximity effect was discovered in the Nb/InAs(100) model system.^{12,13} Given the facility of forming ohmic contacts to InAs and the interest in transport across InAs hetero-interfaces, it is important to understand how typical device processing steps affect the chemical and physical properties of InAs(100) interfaces.

Any insulating layer present at a metal-semiconductor or semiconductor-semiconductor heterojunction interface can cause nonohmic charge transport across that interface, i.e., the formation of a Schottky barrier. Thus, the preparation of metal-semiconductor interfaces usually starts with removal

of surface oxides and other surface adsorbates. Etching the native surface with nonreactive species, such as gas-phase Ar⁺, is a popular method of removing these adventitious species. Physical sputtering with Ar⁺ allows the first few atomic surface layers of a semiconductor to be removed, and under the right conditions it can be highly spatially anisotropic. For example, when combined with spatial masking, Ar⁺ etching can be used to create features with large aspect ratios.¹⁴⁻¹⁷ As attractive as Ar⁺ etching is, however, it cannot be employed if it leads to substantial alteration of substrate properties. In this study, we characterize the Ar⁺-induced damage to the near-surface region of InAs(100), under various etching conditions with the obvious goal of minimizing Ar⁺ damage effects and identifying those conditions which produce an oxide-free, well-formed and reproducible interface.

II. EXPERIMENT

Bulk-grown, (100)-oriented, single-crystal InAs wafers obtained from OMK (Slovakia) are used. They are *n*-type (Sn+Sb) InAs with a carrier concentration of 1.2×10^{19} cm⁻³, as reported by the manufacturer and confirmed by the position of the L_+ collective phonon-plasmon mode in the inelastic light-scattering spectrum. Ion etching is performed in a stainless steel ultrahigh vacuum (UHV) chamber using an ion gun (Commonwealth Scientific Corp.) in a Kaufmann configuration. The base pressure in the chamber is 2×10^{-8} Torr. During the etching procedure, a constant flow of high-purity Ar is introduced, raising the pressure to 2×10^{-4} Torr during etching. Etching is carried out with a voltage and beam current of 75 V and 1 mA, respectively, unless otherwise stated.

^{a)}Electronic mail: bohn@scs.uiuc.edu

^{b)}Electronic mail: lhg@uiuc.edu

X-ray photoelectron spectroscopy (XPS) spectra are collected with a Physical Electronics (PHI 5400) instrument using a Mg $K\alpha$ source. The lines used to evaluate the relative surface elemental concentrations are: O(1s), $E_B \approx 531$ eV; As($3d_{5/2}, 3d_{3/2}$), $E_B \approx 42, 43$ eV; and In($3d_{5/2}, 3d_{3/2}$), $E_B \approx 444, 452$ eV.

The Raman spectra are collected in a near-backscattering geometry. Spectra are excited with an Ar⁺ laser (457.9 nm) using either a cylindrical or spherical lens with irradiances ranging from 2 to 1800 W/cm². A surface photovoltage effect is observed at irradiances, $I > 240$ W/cm² for this doping level at room temperature. Thus, all spectra presented are acquired at $I < 240$ W/cm². A single monochromator (Spex 500M) equipped with a liquid nitrogen cooled charge-coupled device (CCD) camera (Photometrics 200) utilizing a holographic notch filter (Kaiser) to remove unwanted Raman scattering from the laser line is used to collect the Raman signal. Spectra are collected in the $x(y,z)\bar{x}$ configuration, in which scattering from the longitudinal optic (LO) and coupled photon-plasmon modes are allowed from an InAs (100) surface, and the $x(y,y)\bar{x}$ configuration in which only the LO mode is allowed.¹⁸ The transverse-optic (TO) mode is disallowed in both configurations, and its presence is interpreted to signal lattice damage in the near-surface region.¹⁹

III. RESULTS

A. Two mode scattering

Spectra taken in the $x(y,z)\bar{x}$ configuration exhibit an LO phonon (237 cm^{-1}) and the L_- (217 cm^{-1}) and L_+ ($\sim 1150\text{ cm}^{-1}$) coupled phonon-plasmon modes. Electrons confined near the surface in the charge accumulation region (CAR) give rise to unscreened LO phonon scattering, as explained by the uncertainty principle.^{20–22} At these high carrier concentrations, the confined region of the CAR has a spatial extent, $\Delta x \sim 35\text{ \AA}$, which leads to a $\Delta k \sim 1 \times 10^7\text{ cm}^{-1}$. This is much larger than the scattering wavevector for this excitation wavelength, and leads to $q \neq 0$ scattering at the unscreened LO mode frequency.²³ Since the penetration depth of the 457.9 nm probe light of 97 \AA is greater than the width of the CAR, two modes are observed: an LO mode from the CAR and both low-frequency, L_- , and high-frequency, L_+ , coupled phonon-plasmon modes from the bulk. The L_- mode is predominantly phonon-like, while the L_+ mode is principally electronic in character. The position of the L_+ mode can thus be used to indicate the magnitude of the carrier concentration in the bulk.^{24,25}

B. Etch time

Typical bias voltages used in Ar⁺ etching of semiconductors range from 50 V to several kV.^{14–17} In this study, voltages ranging from 75 V to 300 V are used. At a gun voltage of 75 V, the time required to reach a sputtering equilibrium with respect to the surface concentrations must first be deter-

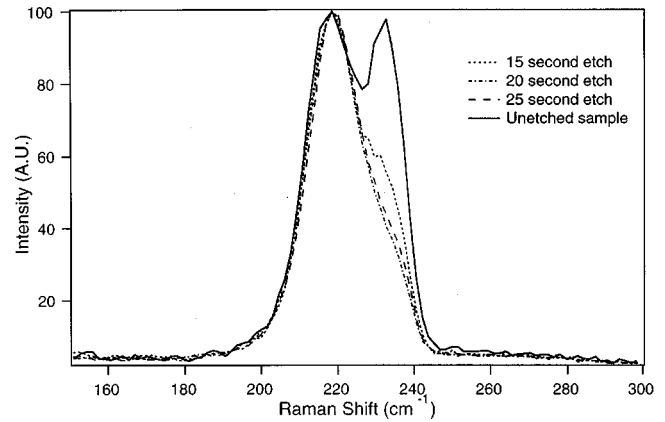


Fig. 1. Inelastic light scattering spectra in the low-frequency region of samples etched at 75 V for varying times. $\lambda_{ex} = 457.9$ nm; $T = 300$ K.

mined. The inelastic light scattering spectra resulting from InAs bulk wafers etched at 75 V for varying times are shown in Fig. 1. It is evident that even at this low bias voltage and short etch time of 15 s, the LO mode intensity is significantly reduced. At longer etch times, the LO mode asymptotically approaches a constant magnitude, and at 25 s is reduced to a weak shoulder on the main L_- peak. This shoulder persists out to etch times of 1 min, indicating that a sputtering equilibrium has been reached by 25 s. Interestingly, XPS studies show that for samples etched at 75 V, the surface oxide remains out to an etch time of 35 s, indicating that any oxide remaining from shorter etch times does not affect the height of the LO mode. It also suggests that the reduction in the LO mode intensity is a physical phenomenon caused by damage to and through the oxide layer, not a chemical phenomenon caused by removal of oxide-related surface states.

The high frequency coupled phonon-plasmon mode derived from InAs etched at 75 V for various times is shown in Fig. 2. The L_+ mode shape and center frequency does not change appreciably. Since the L_+ mode is principally electronic in character, with its center frequency dependent on carrier concentration, the constant position and line shape of

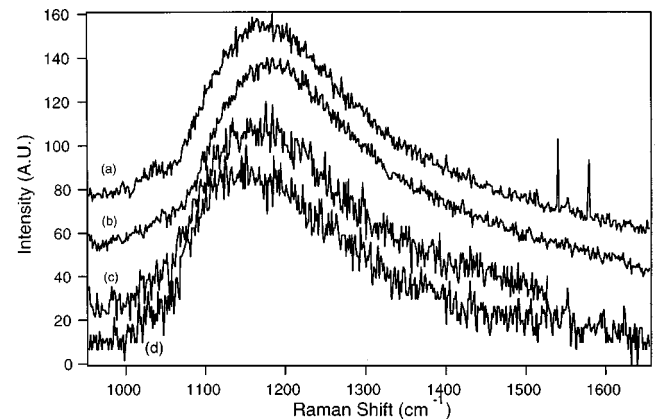


Fig. 2. Inelastic light scattering spectra in the high-frequency region of samples etched at 75 V for varying times: (a) 25 s; (b) 20 s; (c) 15 s; (d) unetched sample. $\lambda_{ex} = 457.9$ nm; $T = 300$ K.

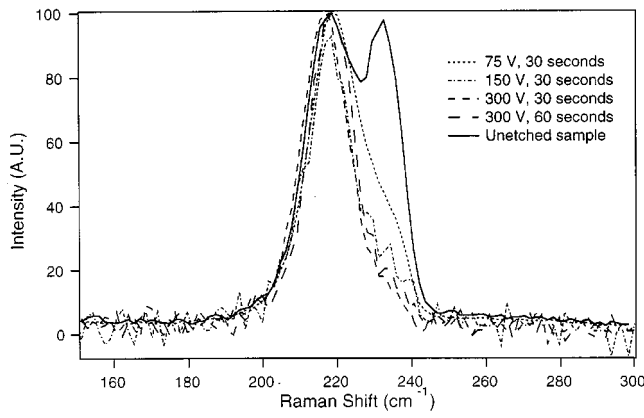


FIG. 3. Inelastic light scattering spectra in the low-frequency region of samples etched at different bias voltages. $\lambda_{ex}=457.9$ nm; $T=300$ K.

the L_+ mode are strong evidence that the damage mechanism does not change the carrier concentration in the bulk region and that the damage produced is confined to the near-surface region.

C. Etch voltage

The low-frequency region of the inelastic light scattering spectra of bulk InAs samples etched for 30 s at varying voltages are shown in Fig. 3. In comparison to the low-frequency spectra of unetched InAs, the LO mode is greatly reduced. While spectral line shape modeling requires both an L_- and an LO contribution for InAs samples etched below 150 V bias voltage, samples etched at higher bias can be fit by the L_- line shape function alone. In addition, in contrast to the behavior at low bias, the high frequency mode changes significantly, moving to higher frequency with increasing etch voltage, as shown in Fig. 4. The behavior of the L_+ mode, indicates an increased carrier concentration in the bulk upon etching at higher bias potentials, most likely resulting from donor states created by the etching process. The coupled plasmon-phonon modes can be used to calculate carrier concentrations using published material constants and taking into account the carrier concentration dependence of the electron effective mass.²⁶ The spectral center frequencies of the L_+ and L_- modes are given by ω_+ and ω_- , respectively, using standard dispersion equations appropriate to a hydrodynamic free electron response,¹⁸

$$(\omega_{\pm})^2 = \frac{1}{2} [(\omega_p^2 + \omega_{LO}^2) \pm \sqrt{(\omega_p^2 - \omega_{LO}^2)^2 + 4\pi_p^2(\omega_{LO}^2 - \omega_{TO}^2)}], \quad (1)$$

where

$$\omega_p = \sqrt{\frac{ne^2}{\epsilon_0 \epsilon_{\infty} m^*}} \quad (2)$$

is the plasma frequency and ω_{LO} and ω_{TO} are the positions of the LO and TO peaks, respectively, n is the electron concentration, ϵ is the dielectric constant of InAs, and m^* is the

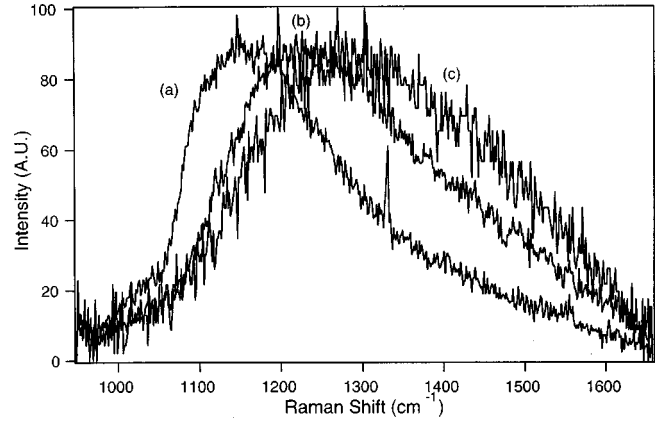


FIG. 4. Inelastic light scattering spectra in the high-frequency region of samples etched at different bias voltages: (a) unetched sample; (b) 150 V; (c) 300 V. $\lambda_{ex}=457.9$ nm; $T=300$ K.

electron effective mass. Table I shows the peak positions and widths with the corresponding calculated carrier concentrations. In addition to the shift to higher frequency with increasing etch voltage, the width of the L_+ modes increases. In the context of the hydrodynamic model this could indicate either a larger dispersion of carrier concentrations in the sample volume probed or increased damping resulting from carrier scattering from etch-induced structural disorder. We note that in all of the above experiments, even those under the most damaging conditions, the InAs retained a mirror-like appearance despite the dramatic changes in the Raman spectra and XPS-derived composition.

D. Annealing

The above results demonstrate that the low-frequency inelastic light scattering spectra are perturbed even under the gentlest etching conditions. At higher bias voltages, damage extends further into the bulk, and donor states, manifested by an increased carrier concentration in the probed volume, are created. In an effort to remove the etch damage, an annealing step is added to the processing protocol. After etching, samples are optimally annealed *in situ* at 500 °C for 12 min. This annealing procedure always returns the L_+ mode to the position and width of the unetched material. At temperatures below 465 °C, no change is observed in the Raman spectra after annealing, while for $T > 500$ °C, whitish spots appear, and the surface is visibly damaged. Even more interesting is

TABLE I. Center frequencies for L_+ modes of InAs etched at different bias voltages.

Etch voltage/V	Center frequency/cm ⁻¹	Peak width/cm ⁻¹	Carrier concentration/cm ⁻³ ^a
75	1150	214	1.3×10^{19}
150	1236	293	1.6×10^{19}
300	1285	349	1.8×10^{19}

^aCarrier concentrations are calculated according to Eq. (1).

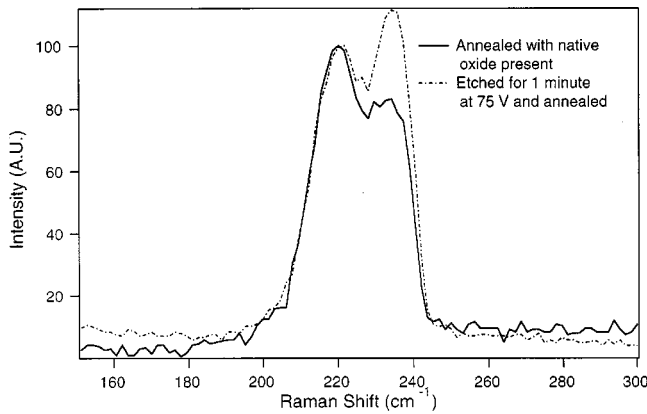


FIG. 5. Inelastic light scattering spectra in the low-frequency region showing the effect of annealing. Samples were etched for 1 min at 75 V to completely remove the oxide, followed by 12 min of annealing in UHV at 500 °C. A sample annealed under the same conditions without first removing the oxide is also shown.

the behavior in the low-frequency region of the Raman spectrum. Figure 5 shows that after an etch-anneal sequence, the LO mode is more intense than that initially observed on an unprocessed sample or from a region that is annealed with the native oxide present, i.e., with the surface masked during etching (compare the LO response of the etched-annealed sample in Fig. 5 to the unetched control in Fig. 1).

XPS results (Table II) obtained on annealed InAs are revealing. Etching according to the conditions described above without subsequent annealing, shows an In/As ratio between 1.4 and 1.6, indicating an In-rich surface, i.e., As is preferentially removed by Ar^+ bombardment. Etching with the InAs held at a temperature at 150 °C produces the largest In/As ratio. Annealing InAs (100) without etching, thereby leaving the native oxide intact, reveals an In/As ratio of 1.2. Etching followed by annealing produces In/As=1.0, indicating a stoichiometric near-surface region. Clearly, dynamic processes involving atom migration and volatilization affect the stoichiometry in the near surface region when InAs is etched with or without annealing, so that composition changes in parallel with changes in the light scattering behavior.

IV. DISCUSSION

The etch time studies clearly show that, after a short induction period, neither the Raman spectra nor the In/As ratios show any dependence on etch time. A sputtering equilibrium is reached within 20 s, even though XPS results

TABLE II. XPS-derived In/As ratios for samples processed under different conditions.

	Unetched	Etched
Unannealed	1.25	1.45 (75 V, 30 s)
		1.6 (75 V, 30 s, 150 °C)
		1.5 (150 V)
		1.5 (300 V)
Annealed	1.2	1.0

indicate the oxide layer is not completely removed at that point. There are several possible explanations for the reduction in LO mode intensity upon etching. One is that Ar^+ etching removes surface states resulting from oxides or surface reconstructions. In the absence of lattice damage in the near-surface region, removing surface states would unpin the surface Fermi level from its position above the conduction band, thereby reducing the magnitude of the band bending and the width of the accumulation region. Since the LO mode Raman signal is assigned to the CAR in InAs, reducing the volume of the CAR would reduce the intensity of the LO mode. However, this mechanism is not consistent with etch-induced changes observed in the high-frequency region. Higher etch voltages cause the L_+ mode to broaden and shift to higher frequencies, indicating the creation of donor states in the bulk. These donor states most likely represent lattice damage-induced states in the bulk. It is difficult to imagine a process which would produce donor states deep in the crystal and leave the near-surface region undamaged. Furthermore, the XPS results in Table II clearly indicate an etch-induced change in surface composition. Such a change in composition would naturally be accompanied by lattice damage. A second possibility involves etch-induced physical damage in the near-surface region. Such damage would disrupt translational symmetry in the unit cells in the near-surface volume where the LO mode originates, leading to fewer unit cells contributing to LO mode scattering. Unfortunately disallowed TO mode scattering, which is taken as evidence of the extent of etch damage,¹⁹ is masked by the L_- mode from the bulk in these n^+ samples. Even in severely damaged undoped crystals TO mode scattering is typically only a fraction of the intensity of the LO mode, so it is much weaker than L_- scattering. A third possibility is that some of the oxide is driven into the substrate during the etch, disrupting the crystal structure in the near-surface region, resulting in fewer unit cells to contribute to the LO mode.

The annealing experiments help distinguish between the latter two cases. When InAs is etched, the LO mode is diminished in intensity, but it is restored upon annealing. In fact, annealing results in an LO mode intensity (relative to the L_- intensity as an internal reference), greater than the LO intensity in either the unprocessed samples (containing a native surface oxide) or the samples annealed with the native oxide intact. Furthermore, the LO intensity in the samples annealed without etching is significantly smaller than that in the unprocessed samples, suggesting that in these samples annealing causes diffusion of oxygen from the surface oxide into the near-surface region reducing the LO scattering intensity. If etching were to drive oxygen into the substrate in sufficient quantities to affect the LO mode height, the annealing step, which results in redistribution of oxygen atoms deeper into the bulk in unetched samples, would not be expected to restore the LO mode intensity. Since the intensity is restored fully upon annealing, it is likely that only a small amount of oxygen, if any, is driven into the substrate during etching. Thus, the reduction of the LO mode upon etching is more likely due to surface damage, which is subsequently

repaired by annealing at 500 °C. This mechanism is also consistent with the behavior of the L_+ mode, which shifts and broadens upon etching, but is returned to its original position and width by annealing. If significant oxygen redistribution into the bulk occurred the L_+ mode would not be expected to return to its original position. Thus, both the LO and L_+ modes are consistent with surface damage which is removed by annealing and inconsistent with spatial redistribution of surface oxide.

This interpretation is also fully consistent with the XPS results. The increased In/As ratio observed in all etched, but unannealed, samples could indicate either As thermal desorption, preferential As removal, or a segregation of As further into the bulk. The observation that the In:As ratio (~ 1.2) observed for annealed, but unetched, samples is smaller than that observed for etched but unannealed samples (~ 1.5) can be interpreted in the context of the formation of the elemental oxides. Reports on GaAs indicate that Ga_xO_y is thermodynamically more stable than As_xO_y . Thus, over time As_xO_y loses its oxygen to Ga atoms and the free As migrates away or desorbs.^{27–29} The thermodynamic considerations are similar in InAs, with the In oxides being more thermodynamically stable than the As oxides.³⁰ Comparing the four possible combinations of etching/annealing to the In/As ~ 1.0 obtained in the etched then annealed samples can then be interpreted in terms of the propensity of each of the processing protocols to remove As. The most dramatic reduction in As is observed in etched, but unannealed samples as would be expected based on relative volatilization of In and As. Unetched but annealed samples show an intermediate In/As ratio, and it is reasonable to postulate that the native oxide is more readily converted to In oxides at the higher temperatures present during annealing, forcing the As out of the near-surface region. Finally we note that annealing under optimal conditions: (a) results in a near-surface stoichiometry identical to theoretical; (b) returns the L_+ mode to its original position and intensity; and (c) produces a significantly increased LO mode scattering intensity.

V. CONCLUSIONS

Ar⁺ etching, under the mildest conditions employed, even before the native oxide is completely removed causes a large reduction in the LO mode intensity. This reduction is due to physical damage to the lattice in the near surface region. Etching at higher voltages causes, in addition to a reduction in the LO mode, formation of donor states and a concomitant increase in carrier concentration in the bulk, as evidenced by changes in the L_+ mode behavior. Annealing previously etched samples at 500 °C: (a) reduces bulk carrier concentrations to levels observed in unprocessed samples, as evidenced by the return of the L_+ to its original position and width, (b) removes etch-induced lattice damage in the near-surface region, as indicated by the LO mode intensity increasing to levels above that in the unprocessed samples, and (c) gives a stoichiometric surface composition. Clearly the formation of the highly conducting interfaces needed for

ohmic contacts requires that etch-induced damage be removed, and annealing at 500 °C is shown to be an effective mechanism for accomplishing this.

ACKNOWLEDGMENTS

This work is supported by the Department of Energy through Grant No. DE FG02 91 ER45439. XPS measurements were performed at the Center for Microanalysis of Materials, Material Research Laboratory at the University of Illinois at Urbana-Champaign which is also supported by Grant No. DE FG02 91 ER45439. T. A. T. acknowledges support from a Fannie and John Hertz Fellowship and an American Chemical Society Analytical Division Fellowship during the course of this research.

- ¹G. R. Bell, T. S. Jones, and C. F. McConville, *Appl. Phys. Lett.* **71**, 3688 (1997).
- ²P. H. C. Magnee, S. G. den Hartog, B. J. van Wees, T. M. Klapwijk, W. van de Graaf, and G. Borghs, *Appl. Phys. Lett.* **67**, 3569 (1995).
- ³G. R. Bell, C. F. McConville, and T. S. Jones, *Appl. Surf. Sci.* **104/105**, 17 (1996).
- ⁴M. F. Millea, A. H. Silver, and L. D. Flesner, *Thin Solid Films* **56**, 253 (1979).
- ⁵H. Yamaguchi and Y. Horikoshi, *Phys. Rev. B* **51**, 9836 (1996).
- ⁶H. U. Baier, L. Koenders, and W. Monch, *Solid State Commun.* **58**, 327 (1986).
- ⁷C. H. Kuan, R. M. Lin, S. F. Tang, and T. P. Sun, *J. Appl. Phys.* **80**, 5454 (1996).
- ⁸X. Y. Gong, T. Yamaguchi, H. Kan, T. Makino, K. Ohshimo, M. Aoyama, M. Kumagawa, N. L. Rowell, and R. Rinfret, *Appl. Surf. Sci.* **114**, 388 (1997).
- ⁹A. Kastalsky, A. W. Kleinsasser, L. H. Greene, R. Bhat, F. P. Milliken, and J. P. Harbison, *Phys. Rev. Lett.* **67**, 3026 (1991).
- ¹⁰A. Kastalsky, L. H. Greene, J. B. Barner, and R. Bhat, *Phys. Rev. Lett.* **64**, 958 (1990).
- ¹¹A. W. Kleinsasser and W. J. Gallagher, in *Superconducting Devices*, edited by S. T. Ruggiero and D. A. Rudman (Academic, Boston, 1990), pp. 325–372.
- ¹²L. H. Greene, A. C. Abeyta, I. V. Roshchin, I. K. Robinson, J. F. Dorsten, T. A. Tanzer, and P. W. Bohn, *Proc. SPIE* **2696**, 215 (1996).
- ¹³L. H. Greene, J. F. Dorsten, I. V. Roshchin, A. C. Abeyta, T. A. Tanzer, G. Kuchler, W. L. Feldmann, and P. W. Bohn, *Czech. J. Phys.* **46**, 3115 (1996).
- ¹⁴G. F. Feng, M. Holtz, R. Zallen, J. M. Epp, J. G. Dillard, E. Cole, P. Johnson, S. Sen, and L. C. Burton, *Mater. Res. Soc. Symp. Proc.* **93**, 381 (1987).
- ¹⁵O. Wada, *J. Phys. D* **17**, 2429 (1984).
- ¹⁶J. B. Malherbe and W. O. Barard, *Surf. Sci.* **255**, 1991 (1991).
- ¹⁷J. M. Epp, J. G. Dillard, A. Siochi, R. Zallen, S. Sen, and L. C. Burton, *Chem. Mater.* **2**, 173 (1990).
- ¹⁸J. Guerts, *Surf. Sci. Rep.* **18**, 1 (1993).
- ¹⁹J. E. Maslar, P. W. Bohn, D. G. Ballegeer, I. Adesida, C. Caneau, and R. Bhat, *J. Appl. Phys.* **73**, 2983 (1993).
- ²⁰Y. B. Li, I. T. Ferguson, R. A. Stradling, and R. Zallen, *Semicond. Sci. Technol.* **7**, 1149 (1992).
- ²¹S. Buchner and E. Burstein, *Phys. Rev. Lett.* **33**, 908 (1974).
- ²²P. Corden, A. Pinczuk, and E. Burstein, *Proceedings of the Tenth International Conference on Physics of Semiconductors, 1970* (unpublished), Vol. 10, pp. 739–745.
- ²³A. Pinczuk and E. Burstein, *Proceedings of the Tenth International Conference on Physics of Semiconductors, 1970* (unpublished), Vol. 10, pp. 727–735.
- ²⁴T. Yuasa, S. Naritsuka, M. Mannoh, K. Shinozaki, K. Yamanaka, Y. Nomura, M. Mihara, and M. Ishii, *Phys. Rev. B* **33**, 1222 (1986).
- ²⁵K. J. Nash, M. S. Skolnick, and M. J. Bass, *Semicond. Sci. Technol.* **2**, 329 (1987).
- ²⁶*Numerical Data and Functional Relationships in Science and Technology*, edited by O. Madelung (Springer, New York, 1987), Vol. 22.

²⁷G. Hughes and R. Ludeke, *J. Vac. Sci. Technol. B* **4**, 1109 (1986).

²⁸M. J. Chester, J. Terrence, and J. A. Dagata, *J. Vac. Sci. Technol. A* **11**, 474 (1993).

²⁹M. Hong, M. Passlack, J. P. Mannaerts, T. D. Harris, M. L. Schnoes, R.

L. Opila, and H. W. Krautter, *Solid-State Electron.* **41**, 643 (1997).

³⁰*CRC Handbook of Chemistry and Physics*, edited by R. C. Weast, D. R. Lide, M. J. Astle, and W. H. Beyer (Chemical Rubber, Boca Raton, FL, 1990).